General methodology using Computational Fluid Dynamics to quantify the power generation potential of large Indian wind farms

Preprint · April 2019

CITATIONS
0

READS
88

1 author:

Nimish Mishra
Indian Institute of Information Technology, Kalyani
28 PUBLICATIONS **19** CITATIONS

SEE PROFILE

General methodology using Computational Fluid Dynamics to quantify the power generation potential of large Indian wind farms

Author – Mishra, Nimish[1,*]

1 = Indian Institute of Information Technology, Kalyani, West Bengal, India,
* = Corresponding author, nimish_bt18@iiitkalyani.ac.in

Abstract:
The Deccan coastline in India has a great potential for wind power generation due to balanced wind speed spread over a long period of time. Most of the large wind farms in India have state-of-the-art wind turbines and are meeting the energy demands of the regions they supply to. Other farms, however, still use old and inefficient turbines and are not able to exploit their full potential of energy generation from wind. India's energy demand is set to increase in the upcoming years. With a broader vision of a major shift to energy production from renewable sources in the near future, it is essential that such inefficiencies in energy production are eliminated. The performance of the state-of-the-art GE 1.5XLE turbine in these regions is quantified by simulations done by Computational Fluid Dynamics, followed by fitting a polynomial regression model to predict the power output for all farms. The comparison of simulation results and existing statistics are used to identify inefficient wind farms.

The findings of this study also suggest that this simulation methodology in general for any turbine modelled, along with land availability, regulations, and economic allowances can help to quantify improvements in the overall energy output of any region from wind energy, by identifying sites in that region where replacement by the newer wind turbine modelled will lead to more power generation. Such replacements shall incur lesser expense than setting up new farms to meet the increasing energy demand and thus serve as important inputs to investors.

Keywords: Wind energy, Wind turbine, Simulation, Regression, Computational Fluid Dynamics, ANSYS

Abbreviations:
IEA – International Energy Agency
Units used in the article-
- m – metre (the fundamental unit of length in the SI system)
- kg – kilogram (the fundamental unit of mass in the SI system)
- s – second (the fundamental unit of time in the SI system)

rad/s – unit for rotational velocity denoted by ω

deg (°) – degree (unit for measurement of plane angle defined such that a full rotation = 360°)

Pa – derived unit of pressure in the SI system

1.0 Introduction

Electricity has become one of the prime requirements of humans. Since many decades, coal and similar natural non-renewable resources have been the centre of power generation in the world. According to the World Coal Association [1], 37% of the global electricity demand is met by coal-fired power plants closely followed by oil, natural gas, and nuclear resources; from figure 1 [1], almost 65% contribution to Global Energy Generation comes from non-renewable resources. Despite the fact that new reserves are being discovered and new technology is being developed to efficiently extract them, the non-renewable resources cannot be utilized for power generation forever as their rate of usage is far higher than the rate of formation[2].

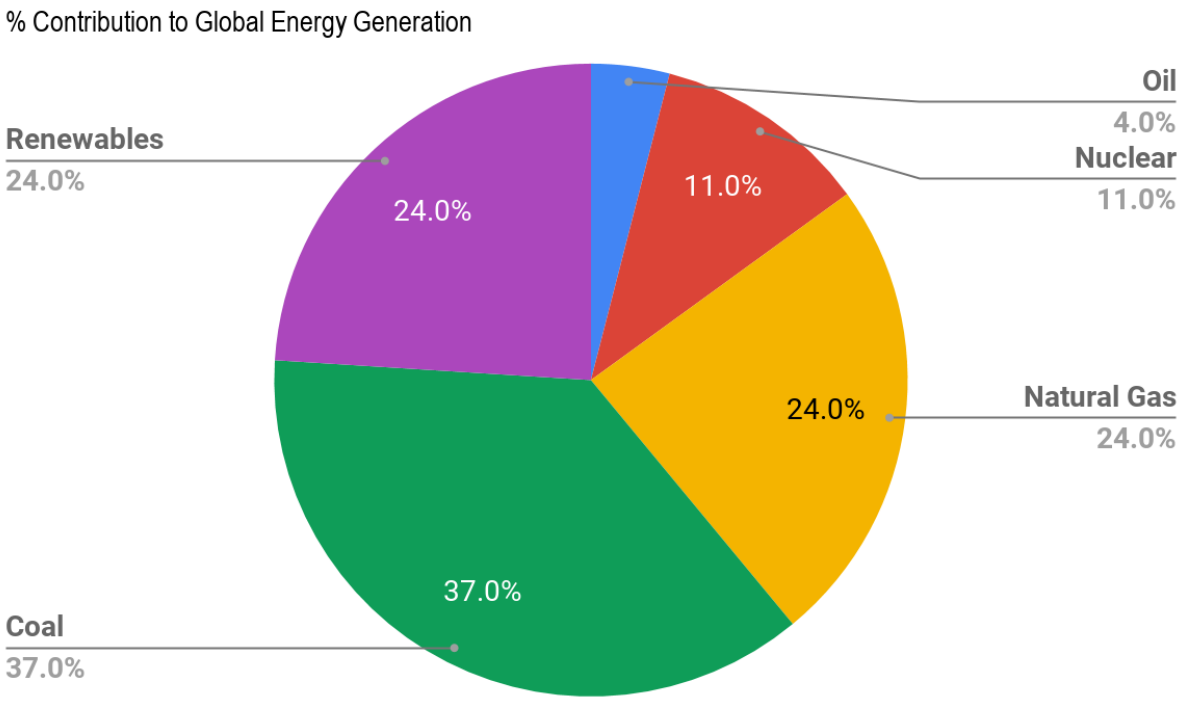

Figure 1: % contribution of each natural resource to Global Energy Generation

This idea has led to a very detailed inquiry in the field of power generation through renewable sources of energy- wind energy, solar energy, hydel energy and tidal energy.

Among these, hydel energy and wind energy have emerged as important sources of energy generation due to their surplus availability and higher efficiencies of energy transformation as compared to other sources such as tidal or solar energy [3], [4]. It is therefore essential to as efficient as possible in power generation from wind and hydel energy.

In the year 2016-17, the electrical demand in India was about 1392 TWh (with a peak demand of 218 GW) [5]. This electrical demand is expected to increase in the coming years as India moves towards a digital and technological revolution. As an estimation, the electrical demand is anticipated to be at least 1915 TWh (peak electric demand of 298 GW) in 2021-22 [5]. Presently, coal, natural gas, and renewable energy contribute to respectively 56%, 9%, and 12% of this demand [5]. The depletion of exhaustible resources in future is ought to increase pressure on the renewable resources.

Advancements in wind power generation technology have led to an increase in the amount of installed wind power generation turbines in many nations [3]. In India, a total of 28700 MW of wind power capacity was installed in the country by the end of December 2016, which increased to a total of 31177 MW by the end of March 2017[5]. However, this capacity is still not enough. According to IEA project, India will need a total of about 327 GW power generation capacity in 2020, and going by the present rate of new installations, it is likely to fall short [5]. Additionally, many states in India are not producing wind power to their full potential. These states have sites with good wind power generation potential, but most of these sites have old and inefficient wind turbines[5]. This study aims to identify such sites and quantify efficient replacements, which are cheaper than the installation of new wind farms, as well as to establish a general, low-cost methodology based on simulation and computational fluid dynamics to quantify the efficiency of existing wind farms in any region by comparison to a model of any wind turbine.

This study collects wind velocity data of the sites having large wind farms, simulates GE1.5 XLE turbines there, fits a polynomial regression model to the data, and quantifies power output. The results obtained are then compared to existing statistics, and it is found that several of these sites are inefficient in power production. Replacements with newer turbines will greatly increase aggregate power output, and will significantly contribute to the increasing usage demands. Such replacements are cheaper than the installation of new wind farms, which involve expenses of testing a potential site for balanced wind speed over a long period of time, development of the farm, and installation of the turbines.

Moreover, if India succeeds in overcoming the aforementioned shortcomings in wind power production, it can generate close to 81 TWh each year by 2020 and close to 174 TWh by 2030 [5]. It is expected that increased reliance on wind energy for power production shall reduce carbon dioxide emissions by nearly 48 million tons in 2020 and nearly 105 million tons in 2030 [5]. In a world of severe environmental crisis, this is a huge reduction in carbon dioxide emission, and it needs to be targeted for the safe future of the environment.

2.0 Methods

2.1 Initial Setup

This study has been done by a simulating a model of a wind turbine at various places along the Deccan coastline and then using a simulation software to quantify the results and compare them with actual power generation statistics to identify inefficient sites. The turbine used for the simulations is GE 1.5XLE turbine, which is one of the most efficient and widely used designs in the wind turbine industry [6].

2.2 Target sites

Choice of a target site for this study involved the creation of a list containing details about the existing wind farms in India, and aggregating weather data at those locations to be fed to the simulation, whose results can then be effectively compared to present statistics. The target sites hence chosen are tabulated in Table 2.

2.3 Turbine Blade Design Methodology

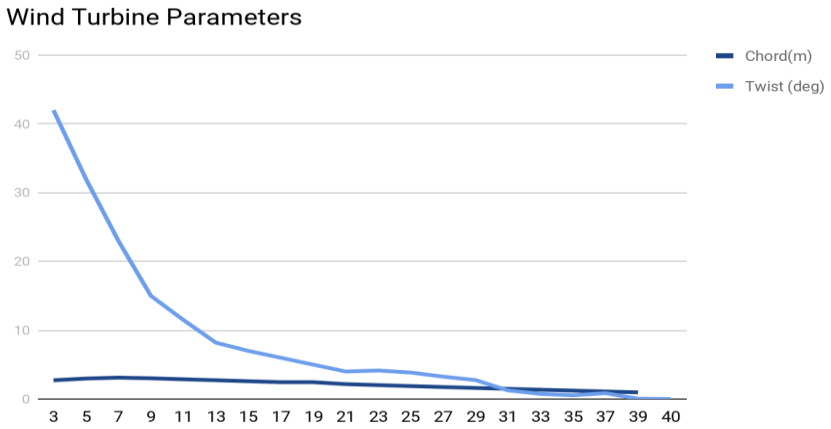

Figure 2 - Graph of (Chord length/radius) and (Twist angle/radius) on the vertical axis against the turbine wingspan on the horizontal axis

The blade model used in this study is 43.2 metres in radius. The hub at the centre is joined to the blade using a cylindrical root section. The entire blade is divided into three blade profiles: S818 (for root), S825 (for body), and S826 (for tip). These airfoils mark the transition of the blade from the cylindrical root to the body and tip [8]. To find the chord length and twist angle of a turbine with a given radius, these design parameters are plotted as functions of wingspan, as depicted in figure 2. It is found that the twist angle and the pitch angle for a blade span of 43.2 metres should be 4 degrees each at the blade tip [7][8].

2.4 Simulation Methodology

There has always been a requirement of prediction techniques that can accurately estimate the performance of multiple turbine installations within a specific local environment operating in a range of local conditions. Earlier, scaled prototypes of the aerofoil to be analyzed were created and placed in large wind tunnels to simulate real-world working conditions. Sensors were placed at different points in the tunnel to record data [9]. This method was costly and time-taking. As an alternative, Computational Fluid Dynamics yields reliable computer-based results that can effectively be applied to real-world conditions. The following procedure is followed in a typical CFD study:

1. The geometry of the simulation is defined based on the real-world structure of the object to be simulated.
2. Meshing is done to divide the volume of the geometry into discrete cells.
3. Governing equations are written down. These model the flow as it happens in the real-world.
4. Boundary conditions are set.
5. Simulation is done for a number of iterations until the solution successfully converges.
6. A postprocessor (like CFD Post) is used to analyze results.

The software used for this study is ANSYS 19.1 [10] because it has several models (inviscid, laminar, k-w, and Spalart Allmaras) which can be compared and used for this study's purpose. Furthermore, ANSYS is a powerful tool for solving the Navier-Stokes equation [11], which is the governing equation for the problem dealt with here (elaborated in section 2.5).

2.5 Underlying Physics involved

To model fluid flow around the blade, ANSYS uses governing equations: continuity equation (derived from the principle of conservation of mass) and Navier-Stokes equation. In order to compensate for the rotation of the blade (and to avoid solving the very complex moving mesh problem due to the rotation of the blade [11]), these

equations are written in a frame of reference rotating with the blade. This is done by inputting into ANSYS the rotational velocity of the rotor which modifies the relative velocity of the wind compared to the blade's velocity and the Reynolds Number (which modifies the aerodynamic performance of the flow around the blades) [11].

The equations hence used are:

1. *Conservation of mass (A form of continuity equation)*

$$\frac{dp}{dt} + \left(\frac{d}{dx} + \frac{d}{dy} + \frac{d}{dz}\right).\rho.v_r = 0$$

2. *Conservation of momentum (Navier-Stokes Equation)*

$$\nabla.(\rho.v_{r.}v_r) + \rho(2\omega \times v_r + \omega \times \omega \times \mathrm{r}) = -\nabla\mathrm{p} + \nabla.\tau$$

where *p* is the momentum, ρ is the density of the fluid flowing in the domain, ω is the rotational velocity of the rotating frame of reference, $\nabla = \left(\frac{d}{dx} + \frac{d}{dy} + \frac{d}{dz}\right)$, r is the radius of the blade and v_r is the relative velocity. To these governing equations are attached the boundary conditions as described in section 2.7, which are the initial conditions helping ANSYS to solve the equations for any point on the geometry. The periodicity assumption- under which tripling the results obtained on one-third of the geometry gives exactly the same results as calculation on the entire geometry- is used to divide the domain into three sectors of 120^o [12]. On this one-third of the geometry, the following parameters are initialized at the beginning of the solution:

- Inlet velocity- The incoming velocity of the wind
- Outlet pressure- 1 atmospheric pressure at the outlet of the flow domain

After completing the previous steps, these differential equations are converted into a set of algebraic equations using the piecewise linear approximation method. The solver inverts these algebraic equations to calculate velocities (in X, Y, and Z directions), momentum, and rotational velocity at the cell centres of the discrete cells formed in the meshing step. The values at the cell centres are then extrapolated to find values at all the points on the geometry.

2.6 Model (Geometry and Meshing)

The geometry of the turbine was created using valuable inputs from [13] and [14].

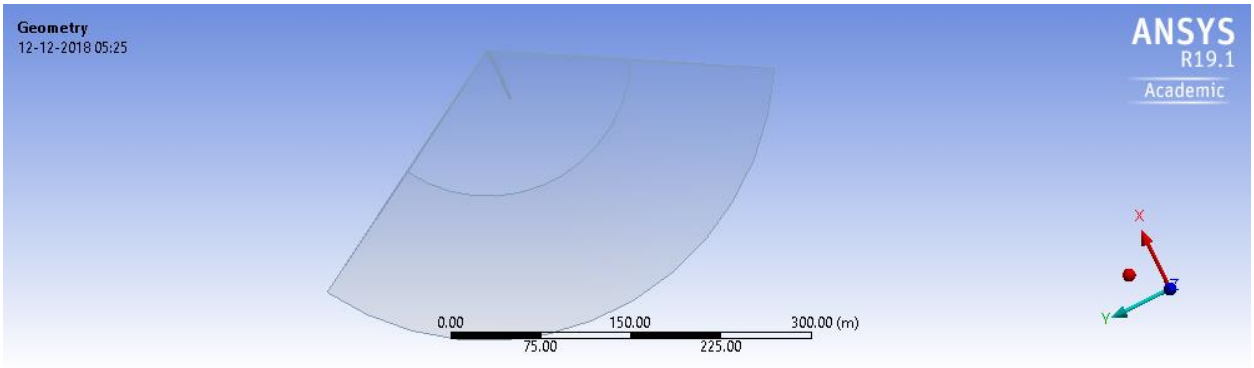

Figure 3: The flow domain of the turbine model. Using the periodicity assumption discussion in section 2.5, only ⅓ portion of the entire circle has been modelled

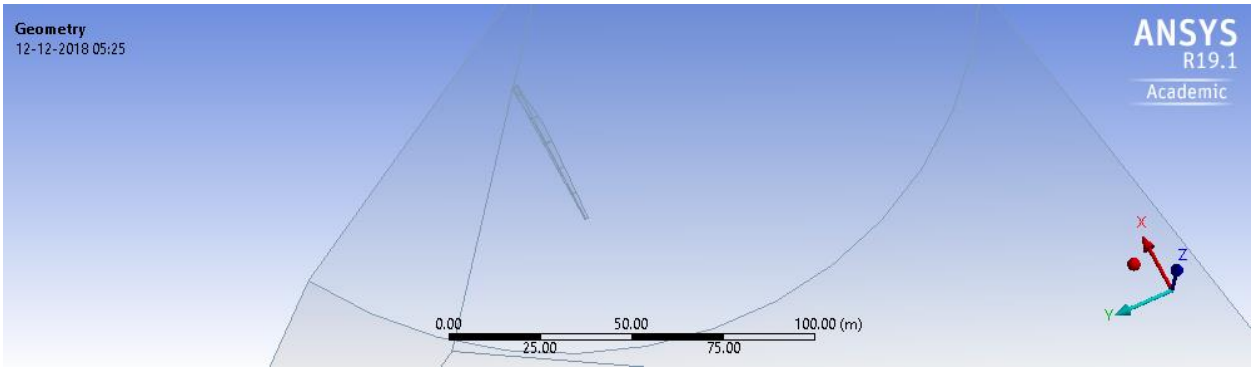

Figure 4: The blade and its segments that have been modelled in accordance with the measurements discussed in Turbine Blade Design Methodology section.

To mesh the above geometry, two different coordinate systems are described: the Global Coordinate system (at the end of the blade) and the User-defined coordinate system (at the centre of the blade). The result is depicted in Figure 5. The demarcation of coordinate systems is done for the *Body sizing mesh control system* that requires a centre for the *sphere of influence* to control the size of discrete cells in the mesh*;* this centre must be set to the point at the center of the blade for optimal results. Hence, defining a new coordinate system is a more judicious choice than picking the original coordinate system and translating it to the centre of the blade.

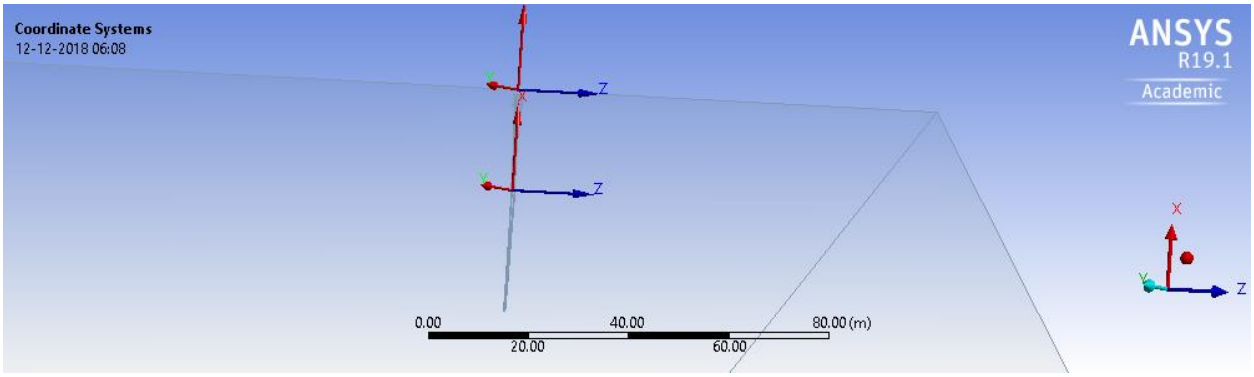

Figure 5: The Global and User-Defined coordinate systems created

Four different mesh control systems were introduced: match control, face sizing, inflation, and body sizing. A range of different combinations of values of these systems was tested. The combination chosen was the one that gave the maximum number of nodes (1834742) and elements (7061100) in the mesh, as well as decent mesh metrics (Skewness and Orthogonal quality are the mesh metrics used in this study [16]). Figure 6 illustrates the systems for the following values:

a. **Match control**: Cyclic transformation
b. **Face sizing:** Element size (5e-2 m); Defeature size (2.5e-2 m); Behaviour (Hard)
c. **Inflation:** Boundary (Blade [*see Named Selection* in section 2.7]); Inflation option(Smooth Transition); Transition ratio (0.272); Max. Layers (10); Growth Rate (1.2); Inflation Algorithm (Pre)
d. Body sizing: Type (Sphere of Influence); Sphere center (**User defined Coordinate system**); Sphere radius (50 m); Element size (1 m).

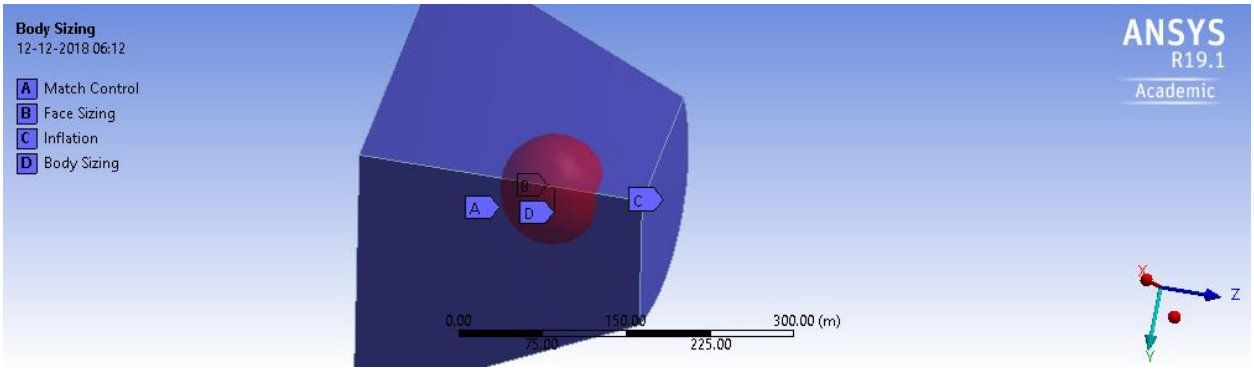

Figure 6: Depiction of Mesh Control systems in the flow domain

The following mesh metrics criteria gave been used in this study (derived from information from [15])

Skewness:

Skewness values: Ranges of *skewness* mesh metric values to judge an element's quality

Mesh quality	Outstanding	Very good	Good	Sufficient	Bad	Inappropriate
Range	0 - 0.25	0.25 - 0.50	0.50 - 0.80	0.80 - 0.95	0.95-0.98	0.98-1.00

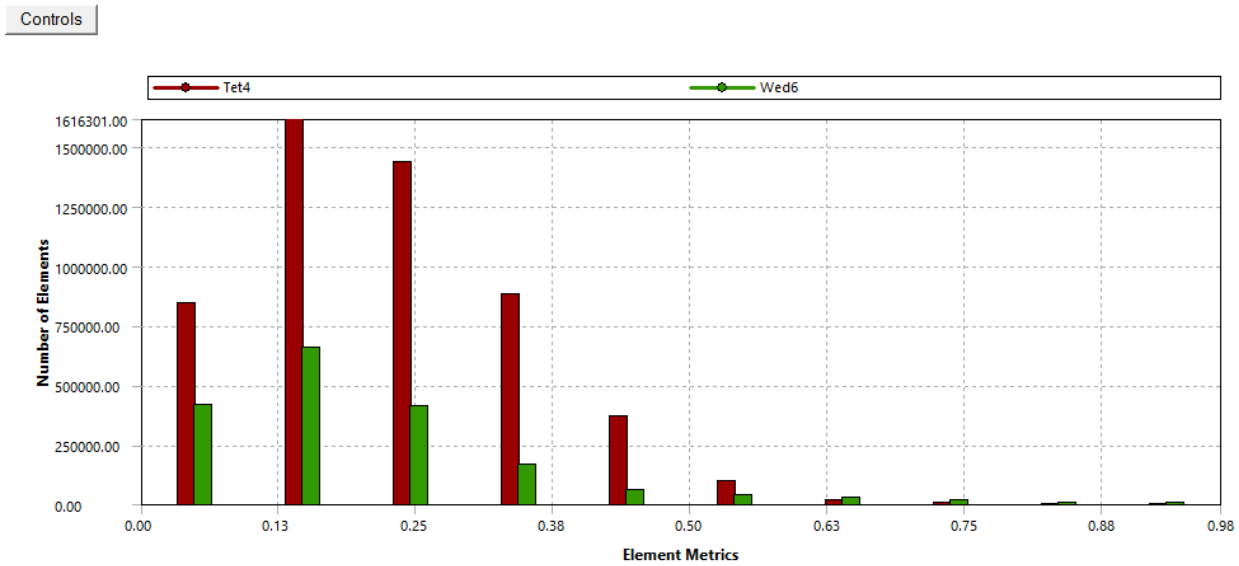

Figure 7: Depiction of number of elements against their Skewness value

From figure 7 and skewness values in the table, nearly all the elements have values less than 0.5, and hence fall in the category: *Very Good* mesh quality. Moreover, the mean of skewness of all the elements is 0.21591 (that falls in the *Outstanding* mesh quality range) and the standard deviation is 0.12625. It is therefore concluded that the mesh is of *very good* quality with respect to the skewness mesh metric.

Orthogonal Quality

Orthogonal Quality values: Ranges of *orthogonal quality* mesh metric values to judge an element's quality

Mesh quality	Outstanding	Very good	Good	Sufficient	Bad	Inappropriate
Range	0.95- 1.00	0.70-0.95	0.20-0.70	0.15-0.20	0.00 1- 0.15	0-0.001

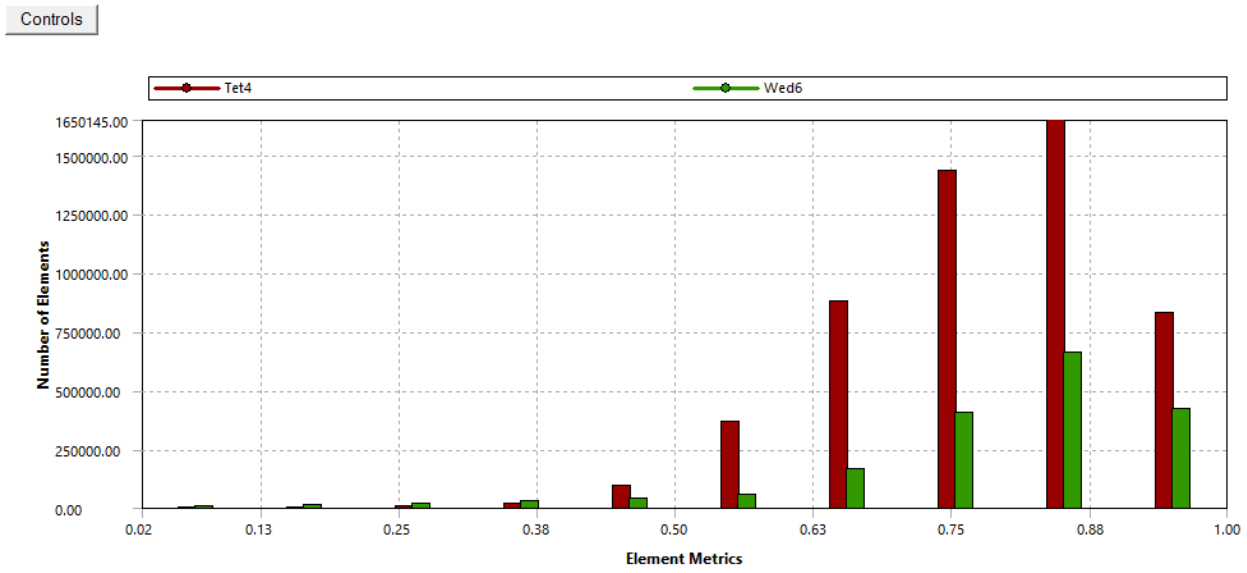

Figure 8: Depiction of number of elements against their Orthogonal Quality

From figure 8 and orthogonal quality table, most elements are above 0.5 and lie in the *Good - Outstanding* region. The mean is 0.78282 and standard deviation is 0.12597. Hence, this mesh is of *very good* quality with respect to orthogonal quality.

2.7 Model Setup for simulation

According to the mesh metrics, the model is of good quality and will closely simulate real-world conditions. To apply boundary conditions to the model, named selections were used, which allow different parts of the mesh to be recognized independently from each other; therefore, specific behaviours can be attached to these independent named selections. The following named selections and boundary conditions were defined for this particular mesh(depicted in Figure 9):
The following boundary conditions were applied to the Named Selections discussed above:

a. **Inlet, Inlet-top:** Both are the velocity inlets. The velocities were described in the absolute frame of reference using separate values for all three coordinate directions (x, y, z). Values entered are tabulated in data in section 3.
b. **Outlet:** This is the pressure outlet. To simulate real-world conditions, a gauge pressure of 0 atm was used. This equals the ideal normal pressure of 1 atm on the outlet.
c. **Period 1, Period 2:** These are the interfaces: the boundaries on which the periodicity condition (as discussed in section 2.5 and in [12]) is applied. This implies calculations done on one-third of the flow domain (120^o) can be tripled to find results for the entire flow domain. This saves precious

computing resource because the number of equations to be solved goes down to one-third, still giving accurate results.

d. **Blade:** Blade is a wall and the fluid flow is considered only *along* its surface.
e. **Fluid-** Fluid is the interior of the fluid flow domain.

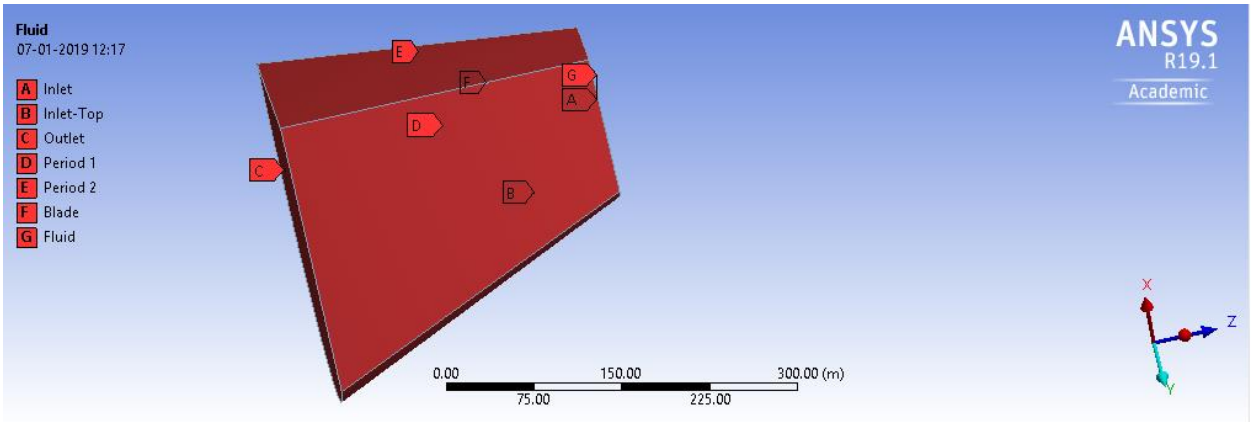

Figure 9: Named selections applied on the turbine geometry

The material used for the simulation was normal air, with ground truth values for density (= 1.225 $kg\ m^{-3}$) and viscosity (= 1.7894e-05 $kg\ m^{-1}s^{-1}$). The cell zone conditions had the *Frame motion* option selected, which allowed manual entry of rotational velocity of the frame of motion. The inputs were taken from data as described in section 3.

ANSYS offers various viscous models to stimulate the real world flow of the fluid under consideration- inviscid, laminar, k-w, and Spalart Allmaras [10]. The inviscid model relies on the inherent assumption that the fluid is perfect (no viscosity and no turbulence) [11]. The laminar model inherently assumes that the fluid flow is turbulence free [11]. Both these models are rejected because they clearly do not conform to the real-world dynamics of fluid flow. On the other hand, k-w and Spalart Allmaras are found to give both accurate and approximately similar results. It is, therefore, safe to interchangeably use either model [11]. For this study, the k-w omega (alternatively named SST k-omega) model is used because it adds two equations (kinetic energy and dissipation) to the Navier-Stokes equation. On the other hand, Spalart Allmaras model is a one equation model, containing only the Turbulence Kinetic Energy equation [18]. Energy dissipation on fluid flow is a ground truth in the fluid dynamics of the real-world. It is, therefore, better for this study to stick to the two-equation SST k-omega model.

From [17], SST k-omega adds the following important equations:

Turbulence Kinetic Energy

$$\frac{\partial k}{\partial t} + U_j \frac{\partial k}{\partial x_j} = P_k - \beta^* k\omega + \frac{\partial}{\partial x_j}\left[(v + \sigma_k v_T)\frac{\partial k}{\partial x_j}\right]$$

Specific Dissipation Rate

$$\frac{\partial w}{\partial t} + U_j \frac{\partial \omega}{\partial x_j} = \sigma S^2 - \beta \omega^2 + \frac{\partial}{\partial x_j}\left[(v + \sigma_w v_T)\frac{\partial \omega}{\partial x_j}\right] + 2(1 - F_1)\sigma_{\omega^2}\frac{1}{\omega}\frac{\partial k}{\partial x_i}\frac{\partial w}{\partial x_i}$$

Before running the simulation, certain residuals were set to describe the tolerance level to judge convergence [19]. The SST k-omega model used the following residuals: continuity, x-velocity, y-velocity, z-velocity, k, and omega. All these were set to 1e-06 (which is considered a safe value in ANSYS to declare convergence [19]). Some other settings used to fasten the process of convergence were:

- *Scheme for pressure-velocity coupling*: Coupled
- Spatial Discretization:
    - *Gradient* - Least Squares Cell Based
    - *Pressure* - Standard
    - *Momentum* - Second Order Upwind
    - *Turbulent Kinetic Energy* - First Order Upwind
    - *Specific Dissipation Rate* - First Order Upwind

Other conditions used were *Pseudo Transient* (under *Transient Formulation*) and relaxing Higher Order terms to speed up calculations.

3.0 Calculation and Data collection

For the turbine's stability, it is mandatory to maintain a reasonable wind tip ratio (when given a certain wind turbine swept area) [20]. The tip speed ratio is defined as the relationship between rotor blade velocity and relative wind velocity. For GE 1.5XLE with a radius of 44.2 m (including the hub offset), a reasonable wind tip ratio is 8.

Considering a certain wind velocity $V\ m\ s^{-1}$(in the negative z-direction). From [20], the equation to calculate the rotational velocity of the rotor given the wind velocity is:

$$\lambda = \frac{\Omega R}{V}$$

Where, λ is the wind tip ratio, λ = 8 was used. Ω is the rotational velocity of the rotor that needs to be calculated. R is the radius of the wind turbine being used (= 44.2 m which is 43.2 m being the radius of the blade and 1m cutoff considering the hub). For different

values of incoming wind velocities V $m\ s^{-1}$, Ω is calculated. In the real world, this implies running the rotor with the calculated rotational velocity in order to give stability to the turbine by ensuring requisite wind tip ratio (~ 8).

The data collected is tabulated in Table 1 (generation of one data point can take varied time depending on the system configuration and hardware. On *AMD A6-7310 APU with AMD Radeon R4 Graphics- 2 GHz* processor and 3.47 GB usable RAM, one data point generation took ~ 3.5 hours).

4. **Results:**

Before the data collected is used for comparisons with existing statistics, several monitors were set up to manually determine any internal bias in the calculation done by the software to check whether the data generated is reliable or not.

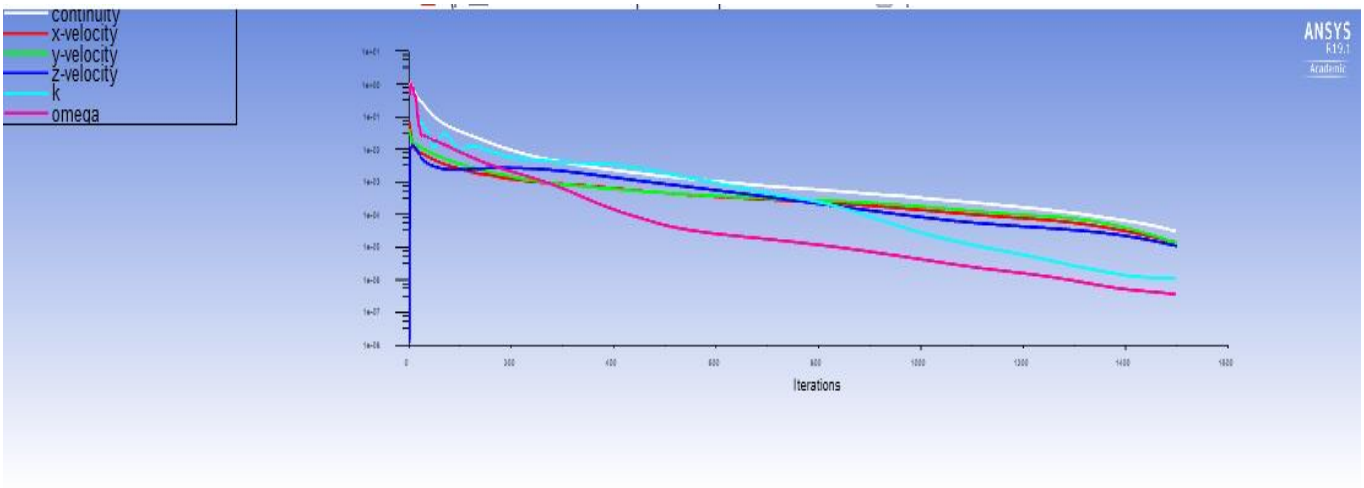

Figure 10: Observing convergence of variables*

* - The variables included in this monitor are: continuity, x-velocity, y-velocity, z-velocity, k, and omega. These converge to the optimum solution as in Figure 11:

iter	continuity	x-velocity	y-velocity	z-velocity	k	omega	report-def	time/iter	
1497	3.1598e-05	1.4237e-05	1.3819e-05	1.1192e-05	1.0795e-06	3.6092e-07	-1.0346e+04	0:00:22	3
1498	3.1383e-05	1.4112e-05	1.3657e-05	1.1100e-05	1.0780e-06	3.5910e-07	-1.0346e+04	0:00:15	2
1499	3.1129e-05	1.3986e-05	1.3496e-05	1.1005e-05	1.0769e-06	3.5727e-07	-1.0346e+04	0:00:07	1
1500	3.0833e-05	1.3861e-05	1.3323e-05	1.0911e-05	1.0758e-06	3.5543e-07	-1.0346e+04	0:00:00	0

Registering ReportDefFiles, ("C:\Users\user\Desktop\nimish\ANSYS Simulations\Wind turbine\Wind Turbine project

Figure 11: Values of variables in Figure 10 after convergence

With respect to the discussion about residuals in section 2.7, all the variables (continuity, x-velocity, y-velocity, z-velocity, k, and omega) have converged significantly [19]. The integral static pressure has also converged to 0 $Pa\ m^{-2}$ as is observed from Figure 12. These suggest that the solution of the simulation is reliable.

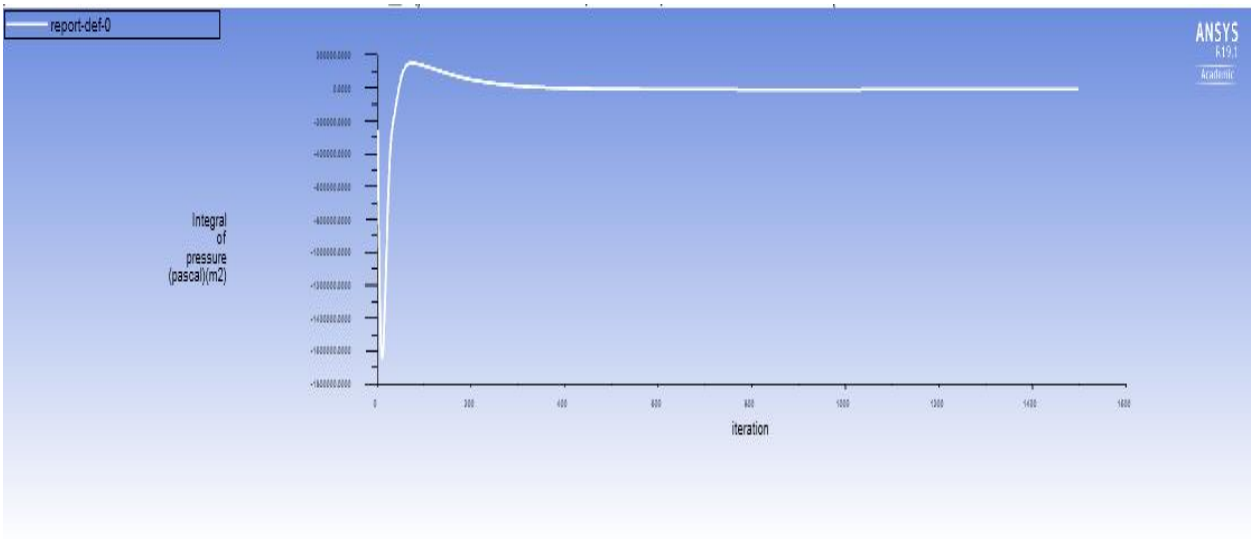

Figure 12: Convergence graph of Integral Static Pressure

Figure 13 shows the mass flow rate report, which calculates the difference between the incoming mass per unit time and the outgoing mass per unit time. From the figure, the mass flow rate is -0.21512808. This implies the simulation adheres to the real world condition where the wind turbine doesn't hold back any mass that enters the flow domain.

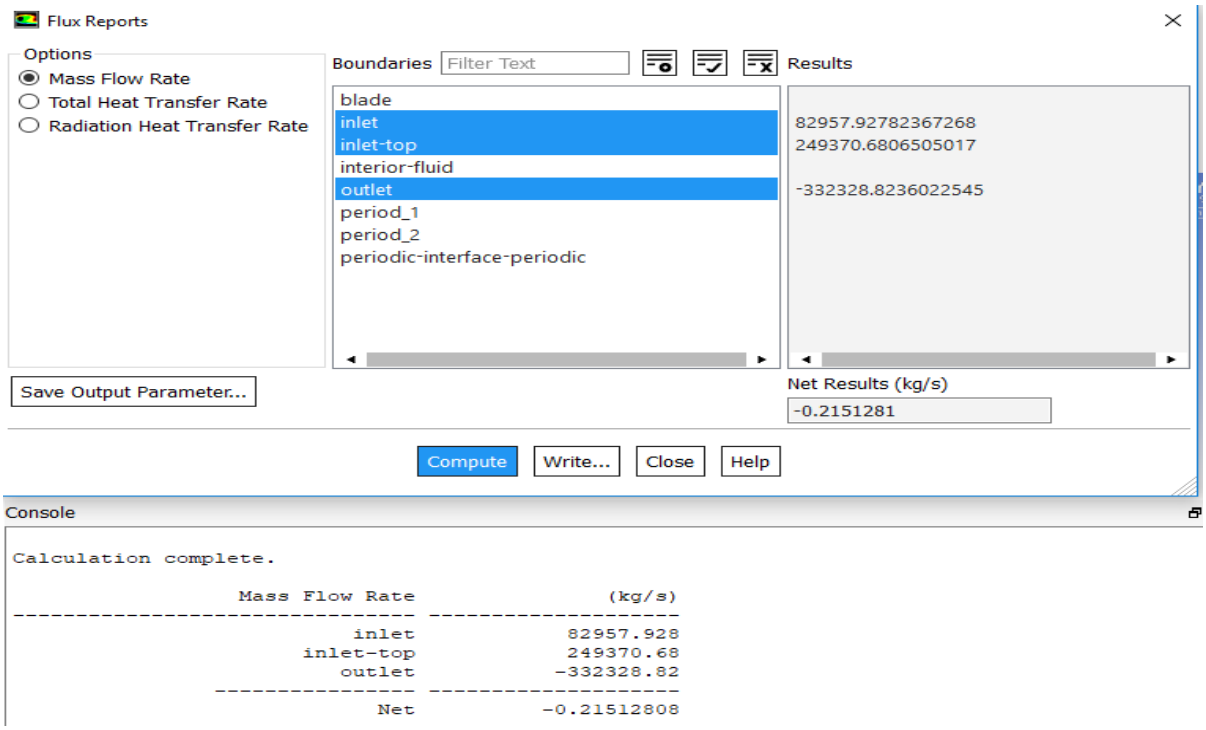

Figure 13: Mass Flow Rate report

The above tests suggest that the simulation has yielded a fairly accurate model of the real world, and that the data in Table 1 can be relied upon. Plotting the dependent (total power output) and the independent (wind velocity) variables as a scatter plot, the following figure is obtained.

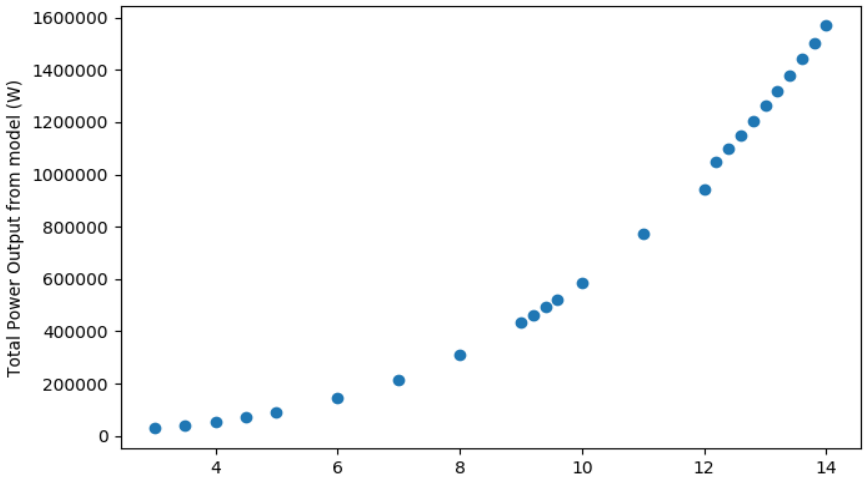

Figure 14: Variation of total power output with wind velocity
(Output rated speed according to model: 14 m/s)

A polynomial regression model is trained on the data collected to output predicted power for any given value of wind velocity (in $m\ s^{-1}$). Polynomial regression is chosen as it is an able alternative to neural networks [23]. Moreover, scikit-learn [24] (a leading python library about various machine learning algorithms) offers a very convenient way to implement polynomial regression. Implementing this involves adding polynomial features based on the input features, viz. wind velocity. Scikit learn offers the *PolynomialFeatures* function under the *sklearn.preprocessing* module that can be used to add the aforementioned features based on the highest degree of the polynomial required. In Python, the process to achieve the same is:

1. Import *PolynomialFeatures* from *sklearn.preprocessing*
2. Scale down the output label (total power output) by a factor of (10^6) to speed up training
3. Apply a degree 2 transformation onto the train data

Post this transformation, *LinearRegression()* module from sklearn was made to fit the training data. The line of best fit was plotted as in Figure 15:

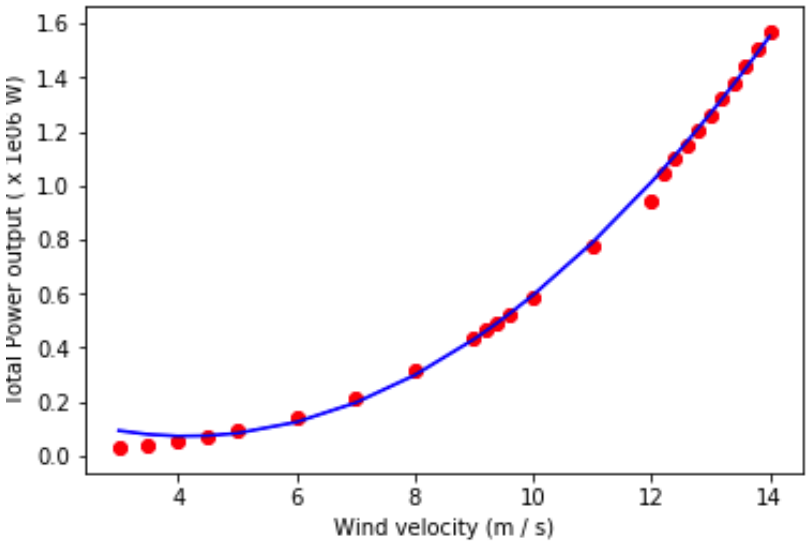

Figure 15: Line of best fit on the training data from section 3

Table 2 has a list of various sites along the Deccan coastline in India (having large scale turbines and reliable source of information about the constitution of the wind farm and wind speed variations in a long period of time) and comparisons with original statistics and the predicted output from the model. The wind velocities considered are the average hourly gusts in the specific region in its most productive period of the year.

5. **Discussion and Conclusion**

Table 2 has quantified the expected power output of the GE 1.5XLE turbines in these regions. Mostly higher values of expected power outputs suggest that these specific sites are not efficient in producing power from wind energy. Replacement of their turbines with the state-of-the-art GE1.5 XLE (or any other turbine of similar design parameters) shall manyfold increase output from these farms, thereby increasing the aggregate power output and moving towards achieving the target power output, as estimated by the IEA project.

Based on the comparison between the results obtained from the simulation and the actual data from the wind farms, it is inferred that expanded use of Computational Fluid Dynamics simulations can be a valuable part of a multidisciplinary effort to truly determine the medium term potential for wind power in any region. Such an effort may also incorporate information on land use availability, inputs on economics, government regulations, as well as compatibility with the regional power grid to estimate the cost of such replacements and provide inputs to potential investors.

Results from the model simulated depend greatly upon the meshing of the model. From the discussion about Figure 7 and Figure 8, it is clear that the present mesh could be tuned even more, which could lead to better results (possibly closer to the actual output rated speed of the GE 1.5XLE turbine- 11.5 m/s). A better mesh quality implies more proximity to real-world output from the turbine. Moreover, data about most wind farms in India and wind speeds in that particular region is hard to gather as the present data is sparse and mostly from unreliable methods. Further research prospects could be to expand on the above observations by gathering data from other regions in India and documenting the results.

This study's data and code used to fit the regression model is hosted on Mendeley Data.

Acknowledgements
The author has received much support from his mother, Mrs. Neelam Mishra, in the preparation and in the proof-reading of the manuscript.

This research did not receive any specific grant from funding agencies in the public, commercial, or not-for-profit sectors.

References

[1] World Coal Association (2013). Coal's role in electricity generation worldwide. Retrieved from link [Last accessed April 26, 2019]

[2] Tathagat D, D. Dod. R. Role of Green Buildings in Sustainable Construction- Need, Challenges and Scope in the Indian Scenario. IOSR Journal of Mechanical and Civil Engineering 2015. Volume 12, Issue 2, Version II. PP 01-09

[3] Arun K.K., Navaneeth V.R, Kumar S.V., Ajay R. Analyzing the Effect of Dimples on Wind Turbine Efficiency Using CFD. International Journal of Applied Engineering Research 2018. Volume 13, Number 6. pp. 4484-4489.

[4] Global Wind Energy Council. Indian Wind Energy (A Brief Outlook). 2016.

[5] Khare V, Nema S. , Baredar P. Status of solar wind renewable energy in India. Renewable and Sustainable Energy Reviews 2013. 27. 1–10. 10.1016/j.rser.2013.06.018.

[6] General Electric Company Limited (2009). GE Energy 1.5MW Wind Turbine. Retrieved from link (Last accessed 26 April, 2019)

[7] Schubel P. J. , R. J. Crossley, Wind Turbine Blade Design. Energies 2012. Volume 5, Issue 9. pp - 3425-3449.

[8] Kumar V. Analyzing the Effect of Dimples on Wind Turbine Efficiency. International Journal of Applied Engineering Research 2018. Volume 13.

[9] Ebert P.R. , Wod D.H., The near wake of a model horizontal-axis wind turbine-I. Experimental arrangements and initial results. Renewable Energy 1997. Volume 12, Issue 3. pp- 225-243

[10] ANSYS Academic (Version: 19.2). ANSYS Student Product. Retrieved from link

[11] Khalil Y., Tenghiri L., Abdi F., Bentamy A. Efficiency of a small wind turbine using BEM and CFD**.** IOP Conf. Ser.: Earth Environ. Sci*.* 161 012028. 2018.

[12] Cornell University (2016). Pre-analysis Wind Turbine Blade FSI. Retrieved from link [Last accessed 26 April, 2019]

[13] Schubel P. J. , R. J. Crossley, Wind Turbine Blade Design Review. Wind Engineering 2012. pp – 365- 388.

[14] Cornell University (2016). Geometry Wind Turbine Blade FSI. Retrieved from link [Last accessed 26 April, 2019]

[15] ANSYS User's FLUENT Guide. Mesh Quality. Retrieved from link. [Last accessed 26 April, 2019]

[16] ANSYS FLUENT best practice guidelines. Mesh Quality. Retrieved from link [Last accessed April 26, 2019]

[17] ANSYS FLUENT guide. SST-k omega model. Retrieved from link .[Last accessed 26 April, 2019]

[18] Spalart P. R. , Allmaras S. R. A One-Equation Turbulence Model for Aerodynamic Flows. *La Recherche Aérospatiale* 1992.

[19] ANSYS User's FLUENT Guide. Judging Convergence. Retrieved from link [Last accessed April 26, 2019]

[20] Schubel P. J. , R. J. Crossley, Wind Turbine Blade Design. Energies 2012. Volume 5, Issue 9. pp - 3425-3449

[21] Central Electricity Authority, Ministry of Power, Government of India. Load Generation and Balance Report. 2011–12.

[22] Central Electricity Authority, Ministry of Power, Government of India. Load Generation and Balance Report. 2012–13.

[23] Cheng Xi., Khomtchouk B., Matloff N., Mohanty P. Polynomial Regression as an Alternative to Neural Nets. arXiv:1806.06850v2 (2018)

[24] Scikit learn documentation. Retrieved from link. [Last accessed April 26 , 2019]

[25] Draxl C., Purkayastha A. , Parker Z. Wind Resource Assessment of Gujarat (India). National Renewable Energy Laboratory. Retrieved from link. [Accessed 26 April, 2019]

[26] Clean Development Mechanism. Lalpur Project Design Document. 2018. Retrieved from link [Last accessed 26 April 2019].

[27] Windpower (Wind energy market intelligence). Lalpur wind farm report. Retrieved from link [Last accessed 26 April, 2019]

[28] Windpower (Wind energy market intelligence). Indian wind farms data. Retrieved from link [Last accessed April 26, 2019]

29. References for wind velocity data:

a. Chinta S., Agarwal A., Raghavendra Rao C. Wind Speed Model for Anantapur District, Western Andhra Pradesh, India. International Journal of Innovative Research in Advanced Engineering (2014). Volume 1, Issue 8.

b. World Weather Online. Monthly Climate Averages. Retrieved from link [Last accessed April 26, 2019]

c. Indiastat. Indiastat Month Wise Mean Wind Speed. Retrieved from link [Last accessed April 26, 2019]

d. Meteoblue weather. Meteoblue Weather history. Retrieved from link [Last accessed April 26, 2019]

Table 1: Data collected from the simulation experiments

TR	WV	TR	Vx	Vy	Vz	ω	Res	PT	VT	ST	TT	Power
8	3	44.2	0	0	-3	-0.5429864253	1.00E-06	-19292.5183	1412.0334	-17880.4849	-53641.4547	29126.5817
7.9	3.5	44.2	0	0	-3.5	-0.633484163	1.00E-06	-22812.069	1853.3428	-20958.7262	-62876.1786	39831.0633
8	4	44.2	0	0	-4	-0.7239819	1.00E-06	-26910.7212	2345.8392	-24564.882	-73694.646	53353.5898
8	4.5	44.2	0	0	-4.5	-0.814479638	1.00E-06	-31559.252	2890.2035	-28669.0485	-86007.1455	70051.0687
8	5	44.2	0	0	-5	-0.90314	1.00E-06	-36934.3151	3466.4971	-33467.818	-100403.454	90678.3754
8	6	44.2	0	0	-6	-1.0859728	1.00E-06	-48906.2675	4814.3395	-44091.928	-132275.784	143647.903

8	7	44.2	0	0	-7	-1.2669683	1.00E-06	-63307.1827	6332.5087	-56974.674	-170924.022	216555.317
8	8	44.2	0	0	-8	-1.447963801	1.00E-06	-79991.4452	8033.2262	-71958.219	-215874.657	312578.688
8	9	44.2	0	0	-9	-1.628959276	1.00E-06	-99147.4963	9910.4693	-89237.027	-267711.081	436090.448
8	9.2	44.2	0	0	-9.2	-1.665158	1.00E-06	-103218.508	10306.864	-92911.644	-278734.932	464137.701
8	9.4	44.2	0	0	-9.4	-1.701357	1.00E-06	-107281.496	10710.37	-96571.126	-289713.378	492905.883
7.9	9.6	44.2	0	0	-9.6	-1.737556561	1.00E-06	-111541.877	11120.463	-100421.414	-301264.242	523463.660
8	10	44.2	0	0	-10	-1.809954	1.00E-06	-120211.922	11961.184	-108250.738	-324752.214	587786.568
8	11	44.2	0	0	-11	-1.99095	1.00E-06	-143910.366	14180.866	-129729.5	-389188.5	774854.844
8	12	44.2	0	0	-12	-2.22	1.00E-06	-159429.523	17458.043	-141971.48	-425914.44	945530.056
7.9	12.2	44.2	0	0	-12.2	-2.208	1.00E-06	-175142.423	17062.353	-158080.07	-474240.21	1047122.38
8	12.4	44.2	0	0	-12.4	-2.2443439	1.00E-06	-180699.119	17568.809	-163130.31	-489390.93	1098361.54
7.9	12.6	44.2	0	0	-12.6	-2.280542986	1.00E-06	-186389.389	18079.169	-168310.22	-504930.66	1151516.07
7.9	12.8	44.2	0	0	-12.8	-2.316742081	1.00E-06	-192018.059	18595.789	-173422.27	-520266.81	1205324.01
8	13	44.2	0	0	-13	-2.352941176	1.00E-06	-197889.309	19113.989	-178775.32	-536325.96	1261943.43
7.9	13.2	44.2	0	0	-13.2	-2.389140271	1.00E-06	-203799.675	19643.795	-184155.88	-552467.64	1319922.68
8	13.4	44.2	0	0	-13.4	-2.425339367	1.00E-06	-209814.637	20179.887	-189634.75	-568904.25	1379785.87
8	13.6	44.2	0	0	-13.6	-2.461538462	1.00E-06	-215824.234	20719.884	-195104.35	-585313.05	1440770.58
8	13.8	44.2	0	0	13.8	-2.497737557	1.00E-06	-222008.191	21268.791	-200739.4	-602218.2	1504183.01
8	14	44.2	0	0	-14	-2.533936652	1.00E-06	-228282.211	21824.091	-206458.12	-619374.36	1569455.39

TR - Wind Tip Ratio
WV - Wind velocity
TR - Turbine Radius
Vx - X component of inlet velocity (m/s)
Vy - Y component of inlet velocity (m/s)
Vz - Z component of inlet velocity (m/s)
ω - the rotational velocity of the rotor in rad/s
Res - the residuals under consideration (discussed above in section 2.7)
PT - Pressure component of the torque (for one blade)
VT - Viscous Component of the torque (for one blade)
ST - Sum of PT and VT (for one blade)
TT - Total torque on the three blades (= 3 $\times$ ST [8] and refer to section 2.7 *Boundary conditions point c* for periodicity assumption.)
Power - Total power output of the turbine (= $TT \times \omega$)

Table 2: Comparison of real-world output and predicted output from the simulation

Site name	Number of turbines [28]	Power Output (MW) [28]	Wind velocity (m/s)[29]	Power output predicted for one turbine (MW)	Total predicted output (MW)	Remarks about site
Anantapur	132	277	12.3	1.08550669	143.2868831	Better site (uses Suzlon S97/2100)
Andra Lake	142	107.6	11	0.78779884	111.8674353	**Can improve with GE 1.5XLE**
Arikhana	7	9.5	13.6	1.43486352	10.04404464	**Somewhat improvement**
Baramsar	31	22.5	12.6	1.16154327	36.00784137	**Can greatly improve with GE 1.5XLE**
Bhakrani	18	14.4	11.2	0.83023828	14.94428904	**Can improve with GE 1.5XLE**
Belgaum	31	24.8	11.8	0.96489137	29.91163247	**Can improve with GE 1.5XLE**
Bhanwad	25	52.5	12.3	1.08550669	27.13766725	Better site (uses Suzlon S95/2100)

Bharmasagar	23	37.9	12.2	1.0607724	24.3977652	Better site(Vestas V82/1650)
Bhogat	7	8.7	12.7	1.18750003	8.31250021	**Nearly the same performance**
Bhuj	34	51	13.8	1.49319496	50.76862864	**Nearly the same performance.**
Budh	20	30	13.6	1.43486352	28.6972704	**Nearly the same performance.**
Burgula	44	37.4	11.8	0.96489137	42.45522028	**Can improve with GE 1.5XLE**
Chakala	146	182.5	13.1	1.29438321	188.9799487	**Can improve with GE 1.5XLE**
Chandgarh	46	92	13.1	1.29438321	59.54162766	Better site (Gamesa G97/2000)
Chilarewadi	50	75	13.2	1.32186804	66.093402	**Nearly the same performance.**
Jaisalmer	59	118	13.6	1.43486352	84.65694768	Better site (Turbines of Inox Wind)
Dhalgaon	130	162.5	13.3	1.34965849	175.4556037	**Can improve with GE 1.5XLE**
Dhule-Nandurbar	60	75	13.5	1.40615623	84.3693738	**Can improve with GE 1.5XLE**
Essar	67	100.5	13.6	1.43486352	96.13585584	**Nearly the same performance.**
Galad	4	5	12.3	1.08550669	4.34202676	**Can improve with GE 1.5XLE**
Gajendragad	25	15	12.7	1.18750003	29.68750075	**Can improve with GE 1.5XLE**
Gudepachgan	63	37.8	11.5	0.89618956	56.45994228	**Can greatly improve with GE 1.5XLE**
Harti	39	31.2	12.2	1.0607724	41.3701236	**Can improve with GE 1.5XLE**
Jangi	40	60	12.7	1.18750003	47.5000012	Better site (Suzlon S82/1500)
Kavadya Dongar	57	57	12.8	1.2137624	69.1844568	**Can improve with GE 1.5XLE**
Kazugumalai	51	40.8	12.5	1.13589213	57.93049863	**Can improve with GE 1.5XLE**

Khandke	135	108	11.3	0.85191642	115.0087167	**Can improve with GE 1.5XLE**
Kondamedapally	68	54.4	12	1.01222065	68.8310042	**Can improve with GE 1.5XLE**
Koralahalli	38	22.8	11.7	0.94168515	35.7840357	**Can improve with GE 1.5XLE**
Kukru	25	50	11.9	0.9884032	24.71008	Better site (Gamesha G97/2000)
Kutch	24	50.4	12.3	1.08550669	26.05216056	Better site (Suzlon G97/2100)
Lahori	46	92	12.7	1.18750003	54.62500138	Better site (Inox Wind DF 100)
Lalpur	63	50.4	12.6	1.16154327	73.17722601	**Can improve with GE 1.5XLE**
Ludarwa	90	76.5	11.8	0.96489137	86.8402233	**Can improve with GE 1.5XLE**
Mahidad	63	50.4	12.1	1.03634372	65.28965436	**Can improve with GE 1.5XLE**
Mamatkheda	67	100.5	12.4	1.1105466	74.4066222	Better site (Regen Powertech Vensys V87)
Mandsaur	36	28.8	12.2	1.0607724	38.1878064	**Can improve with GE 1.5XLE**
Mahidad	12	25.2	12.6	1.16154327	13.93851924	Better site (Suzlon S88/2100)
Panchpatta	24	36	13	1.26720399	30.41289576	**Nearly the same performance (Suzlon S82/1500).**
Periyapatti	66	99	13.6	1.43486352	94.70099232	**Nearly the same performance (Regen Powertech Vensys V77/1500).**
Phoolwadi	33	49.5	13.6	1.43486352	47.35049616	**Nearly the same performance (Regen Powertech Vensys V82/1500).**
Ratlam	85	170	13	1.26720399	107.7123392	Better site (Inox Wind DF 93)
Sadawaghpur	49	61.25	13.4	1.37775455	67.50997295	**Can improve with GE 1.5XLE**

Samana	111	88.8	11.3	0.85191642	94.56272262	**Nearly the same performance**
Tejuva	15	31.5	12.8	1.2137624	18.206436	Better site (Suzlon S88/2100)
Vankusavade	7	7	12.2	1.0607724	7.4254068	**Can improve with GE 1.5XLE**
Welturi	24	50.4	12.2	1.0607724	25.4585376	Better site (Suzlon S97/2100)
Yelisirur	-	-	-	-	-	**GE Turbines already installed**